OPEN

Basilar membrane vibration is not involved in the reverse propagation of otoacoustic emissions

W. He & T. Ren

Oregon Hearing Research Center, Department of Otolaryngology and Head & Neck Surgery, Oregon Health & Science University, 3181 SW Sam Jackson Park Road, NRC04, Portland, OR 97239, USA.

To understand how the inner ear-generated sound, i.e., otoacoustic emission, exits the cochlea, we created a sound source electrically in the second turn and measured basilar membrane vibrations at two longitudinal locations in the first turn in living gerbil cochleae using a laser interferometer. For a given longitudinal location, electrically evoked basilar membrane vibrations showed the same tuning and phase lag as those induced by sounds. For a given frequency, the phase measured at a basal location led that at a more apical location, indicating that either an electrical or an acoustical stimulus evoked a forward travelling wave. Under postmortem conditions, the electrically evoked emissions showed no significant change while the basilar membrane vibration nearly disappeared. The current data indicate that basilar membrane vibration was not involved in the backward propagation of otoacoustic emissions and that sounds exit the cochlea probably through alternative media, such as cochlear fluids.

When environmental sounds enter the ear canal, the air pressure oscillation causes the flexible ear drum to vibrate. This vibration reaches the fluid-filled auditory sensory organ, the cochlea, through the middle-ear bony chain. The stapes vibration at the oval window results in a pressure change in the cochlear fluid. Pressure difference across the cochlear partition causes the spiral basilar membrane (BM) to vibrate. It is commonly believed that this vibration starts at the cochlear base and travels towards the apex[1–6]. As the wave travels, the outer hair cell-based cochlear amplifier generates energy and boosts wave amplitude[7–16], resulting in a sharp peak at the best frequency (BF) location (Fig. 1). When enhancing cochlear sensitivity, hair cell-generated energy can also exit the cochlea and results in sound pressure change in the ear canal, known as otoacoustic emissions (OAEs)[17]. Since their discovery, OAEs have been increasingly used for diagnosing auditory disorders and for studying cochlear physiology. Despite more than three decades of intensive study, the backward propagation mechanism of OAEs remains to be demonstrated.

There are two different theories about OAE reverse propagation. According to the backward BM travelling wave theory, OAE travels along the cochlear partition as a travelling wave in the backward direction[17–21]. In the compression wave theory, OAE exits the cochlea dominantly through the fluid as a compression wave[22–26]. The backward-travelling wave theory is supported by indirect measurements, primarily the delay between the stimuli and the emission in the ear canal. It is commonly believed that the cochlear backward delay is the same as the forward delay, i.e., that the emission delay is twice the forward delay[20,27–30]. To detect the expected backward travelling wave, Ren used a scanning heterodyne laser interferometer to measure BM vibration along the cochlear partition[23]. The results, however, showed that the phase of the BM vibration at the emission frequency progressively decreased with distance from the cochlear base, indicating a forward travelling wave. The delay of the OAE at the stapes was smaller than that at the BM. To confirm this observation, BM vibrations at the emission frequency were measured at two longitudinal locations at sound levels as low as 40 dB SPL (0 dB SPL = 20 μPa)[31,32]. It was found that the phase of the OAE at a more basal location leads that at a more apical location, confirming a forward travelling wave. These results are consistent with the experiment independently conducted by de Boer et al[33].

Recent modeling simulations[34–36] raised the possibility that the emission forward travelling waves observed by Ren[23] were measured at locations apical to the generation place. According to the backward travelling wave theory, a backward travelling wave is required for the reverse propagation of OAEs. The aim of the current experiment was to test this theory by measuring electrically evoked BM vibrations at two longitudinal locations basal to the generation site and by observing postmortem changes in the electrically evoked emission (EEOAE)
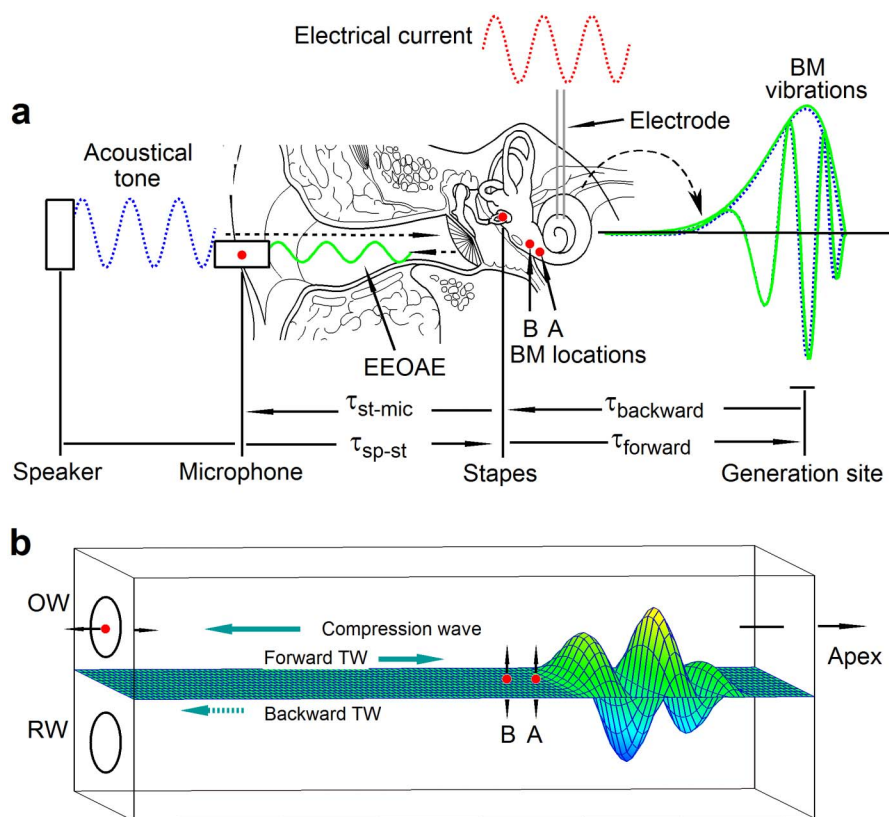
Figure 1 | Diagram illustrating experiment. (a) An electrical current was delivered through a bipolar electrode to stimulate the cochlear partition in the second turn, and electrically evoked BM vibrations were measured at locations A and B in the first turn and the emission in the ear canal respectively. Acoustically evoked BM vibrations were also measured at BM locations A and B. (b) If the emission exits the cochlea as a backward travelling wave, the phase of the BM vibration at location A should lead the BM phase at location B. BM: basilar membrane; EEOAE: electrically evoked otoacoutic emission; τ_{st-mic}: delay from stapes to microphone; τ_{sp-st}: delay from speaker to stapes; $\tau_{forward}$: forward delay; $\tau_{backward}$: backward delay; OW: the oval window; RW: the round window.

and BM vibrations[37–40]. The current results show that the delay of the electrically evoked BM vibration at a more basal location was smaller than that at a more apical location, and either was greater than that of the stapes vibration. Under the postmortem condition, the electrically evoked BM vibration almost disappeared while the EEOAE showed no significant change. These results indicate that the BM vibration was not involved in the backward propagation of the EEOAE, which supports the compression wave theory.

Results

All animals tolerated anesthesia well and survived from surgeries in this study. Due to the invasive experimental procedures and the vulnerability of high-frequency hearing, the productivity for sensitive and complete data is relatively low. Reflective beads were required for measuring electrically evoked BM vibrations with small magnitude. The measured BM locations were determined by the landing points of the beads through the perilymph. The bead positions and the distance between the two measured locations varied across the animals. This prevented us from obtaining averaged data from different animals. The results reported below are typical examples from 4 among 10 animals with sensitive cochleae.

The similarity between the electrically and acoustically evoked BM vibrations is shown in Figure 2. The magnitude and phase of the BM vibrations were measured as a function of frequency from two longitudinal locations with ~350-μm separation at different sound and current levels in a sensitive cochlea. Data in Figure 2 a–c were collected from the more apical location and those in Figure 2 d–f from the more basal location. For either low level tone- or electrical current-evoked responses at a given stimulus level, the BM vibration magnitude

increased with frequency and reached its maximum at the 12.4 kHz for the apical location (Figure 2a) and 15.0 kHz for the basal location (Figure 2d). The peak magnitudes of the electrically evoked vibrations at 10, 33, and 100 μA are comparable to those of acoustically evoked responses at 20, 30, and 40 dB SPL. The pattern of the magnitude-frequency curves for tones is similar to that evoked by currents. The slight difference between acoustically and electrically evoked responses was likely caused by the middle ear transfer function. Across frequencies the magnitude increased linearly with stimulus levels for both currents and low-level tones. This is consistent with a common observation that BM vibrations at low sound levels are approximately linear[41–46]. BM responses at 80 and 90 dB SPL show that the response peak broadened and shifted toward low frequencies. These features, together with the compressive nonlinear growth near the peak, show the healthy status of this preparation. The phase of the acoustically and electrically evoked BM responses is plotted as a function of frequency in Figure 2 b and e. For either tone or current stimulation, the phase progressively decreased with frequency. Since the phase for acoustically evoked responses includes the delay for sound to travel from the speaker to the stapes (Figure 1a), it shows more phase lag than that of electrically evoked responses. After the delay from the speaker to the stapes is removed by subtracting stapes phase from the BM phase, the phase-frequency curves of low-level tone-evoked BM vibration is similar to those of electrically evoked responses (Figure 2 c and f). The phase at 80 and 90 dB SPL led that at low sound levels at frequencies above the BFs, indicating the wave traveled faster at high sound levels. Thus, the data in Figure 2 indicate that, for a given longitudinal location, the electrically evoked BM vibrations are similar to those evoked by acoustic tones in sensitive cochleae.
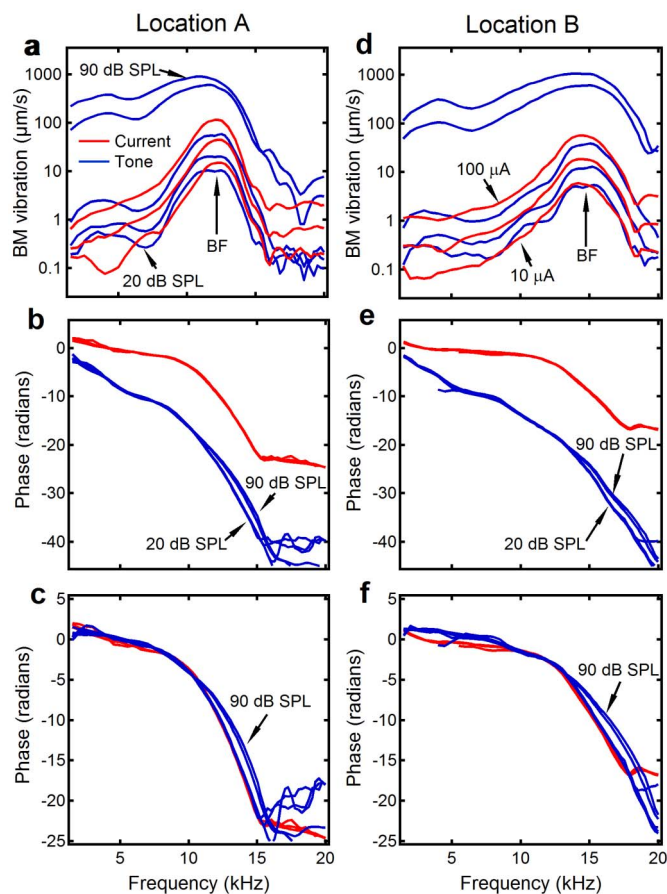
Figure 2 | Similarity between electrically and acoustically evoked BM vibrations. (a and d) For either acoustically or electrically evoked responses at a given stimulus level, the BM vibration magnitude increased with frequency and reached its maximum at 12.4 kHz at location A (panel a) and 15 kHz at location B (panel d). The pattern of the magnitude-frequency curves for low-level tones (blue lines) is similar to those evoked by currents (red lines). BM responses at 80 and 90 dB SPL showed the shifted broad peak and compressive growth. (b and e) Phase progressively decreased with frequency. (c and f) Phase lag of acoustically evoked BM vibrations referred to the stapes was similar to that of electrically evoked responses.
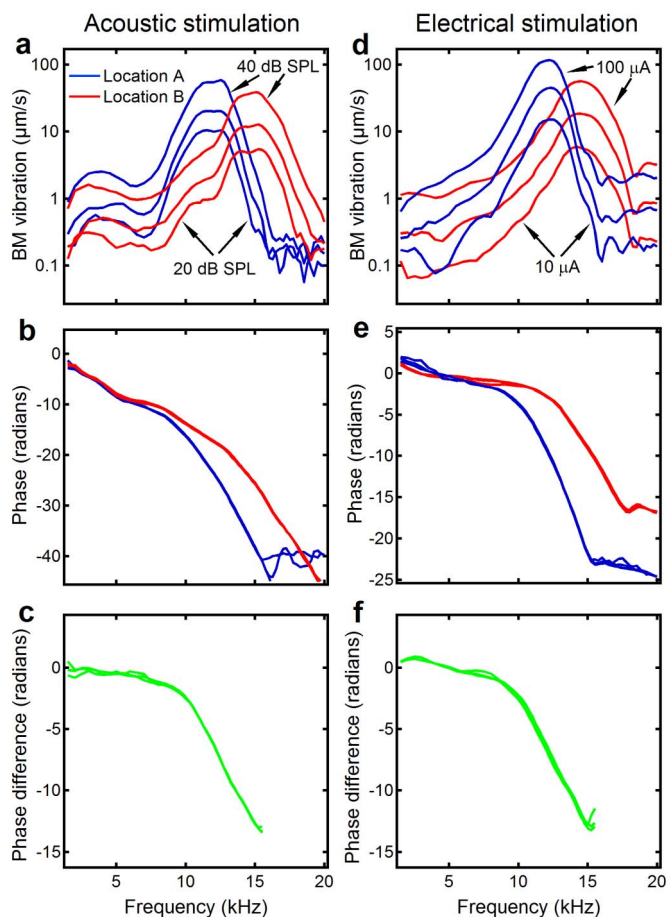

Figure 3 | Comparison of BM vibrations at an apical location with those at a more basal location. (a and d) For either acoustic or electrical stimulation, the peak frequency of the BM vibration at location B is significantly higher than that at location A. (b and e) Phase at location A decreased faster than that at location B. (c and f) The phase difference between the two locations for acoustic stimulation (panel c) is similar to that for electrical stimulation (panel f).

To compare BM responses at an apical location to those at a more basal location, the data from the two locations are plotted together on the same axes in Figure 3. The BM responses induced by acoustic tones are presented in Figure 3 a–c and those evoked by electrical currents are in Figure 3 d–f. For either electrical or acoustical stimulation, the data measured at the more apical location (location A) is indicated by blue lines and those at the more basal location (location B) by red lines. For both stimulations, the BF of the more basal location is significantly higher than that of the apical location. Figure 3 b and e show that phases measured at both locations decreased with frequency at accelerated rates, and the apical location phase decreased faster than those measured at the more basal location. The phase difference between the two locations obtained by subtracting the basal phase from the apical phase is presented in Figure 3 c and f (green lines). Negative phase values indicate that waves traveled in the forward direction. Phase decrease with frequency at an accelerated rate shows the dispersion of the BM vibration. The similarity between Figure 3 c and f indicates that the delay, velocity, and wavelength of the electrically evoked forward travelling wave over the two locations are similar to those for acoustic stimulation[32,47]. Phase difference is slightly greater than zero at the

low frequencies below 5 kHz in Figure 3f. This may be considered an indicator of a backward travelling wave. However, the noisy magnitude response at this frequency range in Figure 3d suggests a limited reliability of these phase values. The small magnitude also indicates that the backward travelling wave, even if it exists, cannot play a dominant role in the reverse propagation of the EEOAE.

To further confirm the wave direction, the cross-correlation coefficient of the electrically induced BM vibrations at the two locations was calculated and is shown in Figure 4. The frequency used in Figure 4 a and b is 10 kHz, which is significantly lower than the BFs (>12 kHz) of the two measured locations. Figure 4 a and b show that the basal location vibrated ~38-μs earlier than the apical location. The delays at other frequencies were calculated and are shown in Figure 4 c, indicating that the delay increased with frequency. Data in Figures 2–4, therefore, show that, as does an external tone, the electrical stimulation of the cochlear partition of the second turn resulted in a forward travelling wave in the first turn.

Different effects of the postmortem change on electrically evoked BM vibrations and EEOAEs are illustrated in Figure 5. The magnitude and phase of the EEOAEs are plotted as a function of frequency in Figure 5 a and b. The BM vibrations measured at the more apical location are presented in Figure 5 c and d, and those at the more basal location in Figure 5 e and f. The measurements were taken at current levels of 10, 33, and 100 μA. Data collected under sensitive
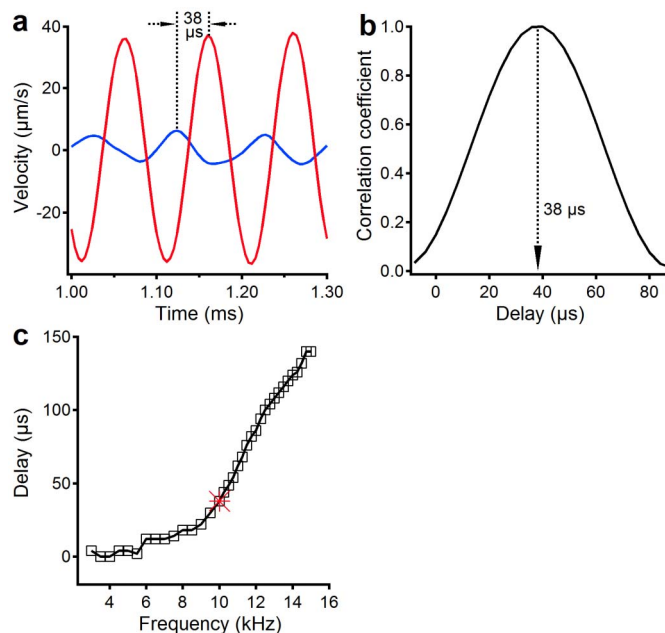
Figure 4 | Cross-correlation coefficient of the electrically induced BM vibrations at two locations. (a) Waveforms of electrically evoked BM vibration at locations A (red) and B (blue) at 10 kHz. (b) The maximum cross-correlation coefficient indicates that location B vibrated ~38-μs earlier than location A. (c) The delay from location B to A increased with frequency. Data were collected at 100-μA current level.

conditions are indicated by solid lines and postmortem data are in dotted lines. Figure 5a shows that the magnitude of EEOAEs increased linearly with the current level, indicated by ~10-dB separation between the curves. The pattern of the magnitude-frequency curves in Figure 5a shows a broad frequency response with peaks and notches. The EEOAE phase decreased with frequency at an approximately constant rate at all levels in the frequency range ~4 to 16 kHz, which indicates a group delay of ~143 μs. This delay consists of delays from the EEOAE generation site to the stapes and from the stapes to the microphone (Figure 1a). The reverse delay of ~50 μs was obtained by subtracting the stapes-microphone delay from the EEOAE delay. Figure 5 d and f show that it took ~438 μs for ear-generated sound to reach the more basal location and ~502 μs to arrive at the more apical location. In contrast to the EEOAEs, the magnitude-frequency functions of BM vibrations measured at both locations under the sensitive condition show sharp peaks at the BFs. Under the postmortem condition, EEOAE showed no significant change, while the BM vibration completely disappeared near the BFs. Thus, the data in Figure 5 indicate that the BM vibration is not required for backward transmission of the EEOAE, and that the EEOAE arrives at the stapes earlier than at a BM location.

Discussion

To demonstrate backward travelling wave, the BM vibrations have to be measured at more than one longitudinal locations basal to the emission generation site. In our previous experiments, the BM vibrations were measured at distortion product (DP) frequency 2f1–f2 when primary tones f1 and f2 (f2 > f1) were presented. Because of the small longitudinal extent of the f1 and f2 travelling waves[48,49] and the cochlear frequency-location map[50], the DP can be detected only from longitudinal locations basal to the f2 place with a limited spatial separation. In the current experiment, the expected backward travelling wave was measured at BM locations far from the emission generation site. This was achieved by electrically stimulating a small region of the cochlear partition at the second turn when the BM vibration was measured in the first turn.
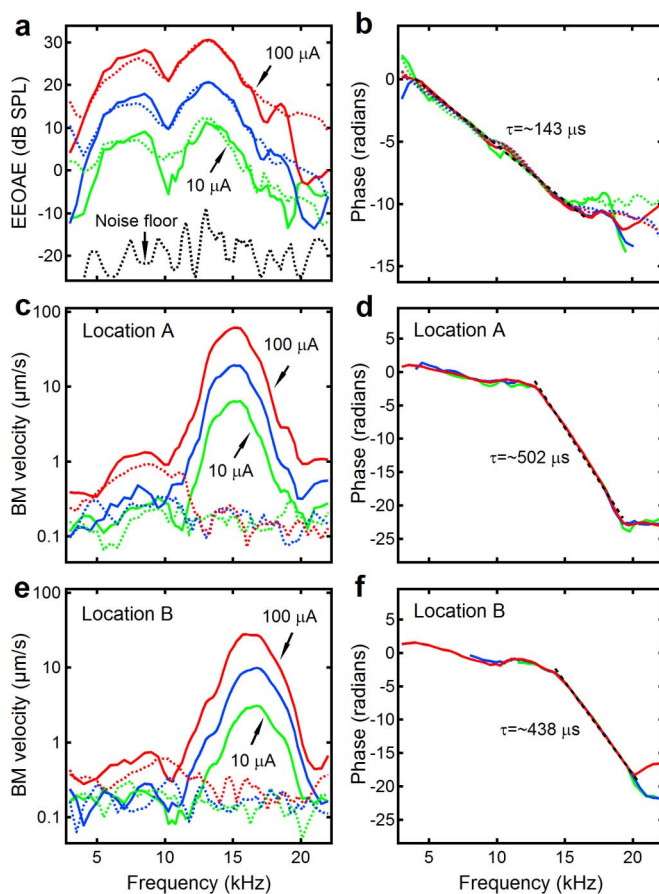

Figure 5 | Electrically evoked BM vibrations and EEOAEs measured under sensitive (solid lines) and insensitive (dotted lines) conditions. (a) Magnitude-frequency curves of EEOAEs show a broad frequency response and linear growth. (b) The EEOAE phase decreased with frequency at an approximately constant rate at the frequency range from ~4 to 16 kHz, which indicates a group delay of ~143 μs. The reverse delay of ~50 μs was obtained by subtracting the stapes-microphone delay from the EEOAE delay. (c–f) The magnitude and phase of electrically evoked BM vibrations at locations A (panels c and d) and B (panels e and f). Phase data in panels d and f show a delay of ~438 μs at location B and ~502 μs at location A. Under the postmortem condition, EEOAE showed no significant change, while the BM vibration disappeared near the BFs. Postmortem BM phase was random and is not shown.

When a sinusoidal electrical current passes through the cochlear partition, an electrical field is created in the tissues. The electrical gradient results in a transmembrane potential change in the sensory outer hair cells. These cells consequently change their length through somatic motility[11] and generate energy through hair-bundle motility[51,52]. Those cellular forces deform the organ of Corti and result in the vibration of the cochlear partition[40,53,54]. The electrically evoked vibration can propagate from its generation site near the electrode toward the apex as does an external sound[55]. The vibration can also propagate toward the cochlea base and result in stapes vibration. The middle ear transforms the stapes vibration into sound pressure change in the external ear canal, i.e., the EEOAE[37].

Since the EEOAE can provide information about the outer hair cell motilities and can be generated locally, it has been used for studying the cochlear amplifier and wave propagation inside the cochlea[54,56]. As for acoustically evoked OAEs, the backward propagation mechanism of EEOAEs is not clear.

To test the hypothesis that the EEOAE exits the cochlea through the backward travelling wave, it is critical to ensure that the electrical

current is delivered to a small region in the second turn. A bipolar electrode and an optically isolated current stimulator were used to restrict currents in this study. In contrast to the glass scala media electrode, flexible bipolar electrodes allowed adjustment of the animal head position for the BM vibration measurement without disturbing the electrodes. Since the tips of the electrode were on the lateral walls of the scala media and the scala tympani through two bony holes, and electrical conductance of the cochlear fluids is relatively high, the current should have passed through the cochlear fluid and stimulated the outer hair cells. This was confirmed by the fact that the current injection through the bipolar electrode resulted in the EEOAE and BM vibration. The use of an optically isolated constant current source ensured that the current flowed only through tissues near the electrode tips without spreading to the cochlea base. To determine whether the bipolar electrode had spatial selectivity similar to that of the scala-media glass electrode, the acoustically evoked cochlear microphonic potential was measured using the two different electrodes at the same longitudinal location in three animals. The same magnitude responses and the identical phase patterns in Figure 6 indicate that the two electrodes had a similar spatial selectivity. The dominating low-frequency CM response below 4 kHz indicates that the electrical current delivered through the bipolar electrode did not spread to the high frequency region in the first turn. Since the motility of outer hair cells is as fast as the upper limit of the audible frequency[57], and since the electrical current is not subject to the filter as is an acoustic stimulus , the electrically evoked vibration served as a local broadband mechanical stimulus near the electrode.

The main findings of the present experiment include that electrically evoked BM vibrations measured at two longitudinal locations are similar to those induced by acoustic tones (Figure 2). As acoustically evoked BM vibrations, at a given frequency, the phase of the electrically evoked BM vibration at a more basal location led to phase measured at a more apical location (Figure 3). Similarly, the electrically evoked stapes vibration occurred earlier than the BM vibration (Figure 5). EEOAEs showed a broad frequency response (Figure 5a) while electrically evoked BM vibrations were sharply tuned (Figure 5 c and e). Like low-level tone-induced BM vibrations, electrically evoked BM vibrations decreased dramatically or disappeared in insensitive cochleae while the EEOAE showed no significant change (Figure 5). Thus, this experiment did not detect the widely expected backward travelling wave at basal locations far from the emission generation site. Since the data showed the electrically evoked forward travelling wave, spectral difference between the EEOAE and BM vibration, and the existence of the EEOAE under the postmortem condition, the BM vibration likely was not responsible for the backward propagation of the EEOAE.
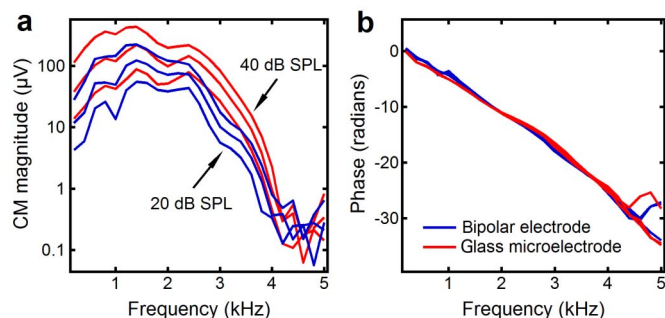
These results are consistent with previous findings that the electrical stimulation of the cochlear partition evoked OAEs[37] and acoustic-like BM vibration[40,53]. The electrically evoked forward travelling wave was also shown by the suppression tuning curve of the electrically evoked compound action potential[58], and by canceling the electrically evoked distortion product OAEs[55]. What is new in the present experiment is the demonstration of the electrically evoked forward travelling wave at longitudinal locations basal to the emission generation site and the difference of the postmortem change on the EEOAE and the electrically evoked BM vibration. The main advantages of this study include that the BM vibrations were measured at basal locations far from the generation site and that the relationship between the BM vibration and EEOAE can be observed under sensitive and insensitive conditions. These were achieved by taking advantage of the fact that the generation site of EEOAEs does not move with frequency[59] and that EEOAEs exist in the passive cochleae[39]. Although the phase transfer function of the BM vibration commonly measured at a single longitudinal location can quantify the delay of the wave, it provides no information on the wave direction[13]. In the present experiment, the wave direction was unambiguously shown by the phase difference between the two longitudinal locations.

While the current result is not consistent with the backward travelling wave theory, it suggests that a fast mechanism is responsible for the backward propagation of the emission. It is possible that the electrically evoked local vibration can travel through the cochlear partition, fluid, or other tissues. The transmission efficiency through these media should be determined by the physical property of the tissues and the anatomy of the cochlea. In mammalian cochleae, there is no direct connection between the cochlear partition and the stapes. For acoustical stimulation, the stapes vibration is converted into the BM vibration through the cochlear fluid. Even if an electrically evoked vibration could reach the basal part of the BM, it should pass through the fluid to vibrate the stapes. Therefore, the fluid pressure wave is required for the emission to exit the cochlea. The remaining question is what is the extent of the fluid compression wave along the cochlear length. It was found that a low-level 16-kHz tone-induced forward travelling wave distributed over only a 600-μm region along the cochlear partition in gerbil[48]. A similar result was reported recently by Fisher et. al in chinchilla[60]. If the backward travelling wave has a longitudinal pattern identical to that of a forward travelling wave but in the reverse direction, the fluid compression wave should be responsible for the emission backward transmission at least from the basal end of the travelling wave (~300 μm from the BF place) to the stapes. When a current passed through the organ of Corti near the electrode in the second turn, the outer hair cells in the electrical field generated forces through somatic and/or hair-bundle motility. These forces resulted in a pressure wave in the fluid, which consequently induced the stapes vibration and a forward travelling wave. Due to the speed difference between the fluid compression wave and the travelling wave, the stapes vibrated earlier than the BM. The normal BM travelling wave relies on functional mechanoelectrical transduction and electromechanical transduction of outer hair cells[13,15]. Upon death, the endocochlear potential decreased, which disabled mechanoelectrical transduction and the cochlear amplifier[61]. The lack of cochlear amplification caused the BM response to low-level tone to decrease. However, as in isolated outer hair cells, electromechanical transduction, i.e., electromotility[11], remained functional in the passive cochlea[39], which was driven by injected current to generate EEOAEs. Therefore, the electrically evoked BM vibrations decreased dramatically under the postmortem condition while the emission showed no significant change.

Using theoretical and experimental approaches, Reichenbach et al. recently showed that mechanical energy can be transmitted by wave along Reissner's membrane and its role in backward transmission of otoacoustic emissions[62]. The Reissner's membrane may play a similar

Figure 6 | Acoustically evoked cochlear microphonic potentials at 20, 30 and 40 dB SPL. (a) The magnitude responses recorded through the scala media microelectrode (red lines) are similar to those recorded using the bipolar electrode (blue lines). (b) Phase curves recorded using the microelectrodes overlap with those recorded using the bipolar electrode. CM: cochlear microphonic potential.

role in the backward propagation of the electrically evoked emission. The phase lag of Reissner's membrane wave, however, appears inconsistent with the fast backward propagation of the electrically evoked emissions.

In summary, this experiment shows that the electrical stimulation of the cochlear partition in the second turn evokes broad-band emission and sharply tuned forward travelling wave in the first turn. Electrically evoked stapes vibration occurs before the BM vibrates. As in sound-induced responses, electrically evoked BM vibration disappears under the postmortem condition while the emission remains. These results indicate that BM vibration is not involved in the backward propagation of electrically evoked emissions.

Methods

Twenty-seven young healthy Mongolian gerbils of 50 to 80 grams were used in this study. The care and use of the animals were approved by the Oregon Health and Science University Institutional Animal Care and Use Committee. The surgical procedures and laser interferometry were described in previous studies[48,63]. Ketamine (80 mg/kg) and xylazine (10 mg/kg) was injected intraperitoneally for initial anesthesia and a half of the initial dose was administered as needed. The animal was wrapped in a heating blanket and the rectal temperature was maintained at $38 \pm 1°C$. A tracheotomy was performed and the animal was kept freely breathing through a ventilation tube inserted in the opened trachea.

After the animal's head was firmly attached to a custom-made head holder, the left auditory bulla was exposed and opened through a ventro-lateral approach. The stapedius muscle was sectioned to eliminate the acoustic reflex. The round window membrane was removed with a tiny hook made of a tungsten micro electrode. A few 20-μm diameter gold-coated glass beads were positioned onto the BM at a radial location 60–90 μm from the osseous spiral lamina. The opened round window was partially covered with a piece of glass cover slip to avoid optical distortion at the air-water interface and to maintain low acoustic impedance of the window. Stapes vibration was measured from the anterior crus. The object beam from a heterodyne laser interferometer was focused on a reflective bead through an infinitely corrected long working distance objective lens (Mitutoyo M Plan Apoxzo, 20×, NA 0.42; Mitutoyo, Japan). The light reflected from the vibrating bead was sent back to the laser interferometer. The Doppler frequency shift was detected by a frequency demodulator and converted into the voltage output. Magnitude and phase of the BM vibration were measured using a custom-built data acquisition system. The propagation delay from the more basal to more apical location was determined by the maximal cross-correlation coefficient of the electrically induced responses at the two locations. The cross-correlation coefficient was calculated using the Correlate operation of a signal analysis program (Igor Pro 6.2.2.2, Lake Oswego, OR). A computer-controlled three-dimensional positioning system was used for focusing the laser beam and for measuring the distance between the beads[48,49].

EEOAEs were evoked by electrical stimulation of the cochlear partition in the second turn. To restrict the current spread, a bipolar electrode was used to deliver electrical currents. The electrode was made of two pieces of 2T (~50 μm in diameter) Teflon-insulated platinum-iridium wire. About 0.05-mm isolation layer was removed from the electrode tips to maintain impedance below 500 kΩ at all stimulus frequencies. Two ~50-μm holes were made using a micro drill in the bony walls of the scalae media and tympani at a single longitudinal location. Great care was taken to avoid damaging the spiral ligament and stria vascularis. The surface of the cochlea was kept dry to minimize the current bypass between the two wires. After the electrodes were fixed to the bony edge of the opened bulla with dental cement, the animal's head was adjusted for BM vibration measurement. The current level was monitored by the voltage across a 1-kΩ resistance connected in serial in the output circuit of the constant current stimulator. The locations of the BM vibration measurement and the electrical stimulation are illustrated in Figure 1. When the scala media glass microelectrode was used for microphonic potential measurement, a Ag/AgCl ground electrode was placed in the neck soft tissues.

An electrostatic speaker (EC1, Tucker-Davis Technologies, Alachua, FL) was used to generate acoustic stimuli. The sound delivering tube from the speaker was connected to the stainless-steel port at the back of an Etymotic 10B+ microphone (Elk Grove Village, IL), which was coupled to the ear canal through a speculum. The sound system was calibrated using a 1/8-inch B&K microphone. To minimize electrical crosstalk, the Etymotic microphone was electrically shielded and grounded. Tucker-Davis Technologies System 2 was used for signal generation and data acquisition. The stimulus level was controlled by a computer via a programmable attenuator. Stimulus frequencies were varied from 500 Hz to 25 kHz in 500-Hz steps. Data were collected at sound levels from 10 to 90 dB SPL (0 dB SPL = 20 μPa) in 10-dB steps. The sinusoidal constant current was delivered by an optically isolated current source, with sensitivity of 100 μA/volt. Currents at 10, 33 and 100 μA rms were used for the EEOAE and BM vibration measurements.

In preliminary experiments, auditory compound action potential (CAP) was measured to monitor the cochlear condition. To ensure sensitive data, the measurements were completed in less than 4 hours without recording the CAP in most experiments. In those animals, cochlear sensitivity was evaluated by compressive nonlinearity of the BM vibration[64]. The data reported here were selected from 10 animals showing >30-dB compression over sound levels from 20 to 90 dB SPL.

1. von Békésy, G. *Experiments in Hearing.* (McGraw-Hill, 1960).
2. Peterson, L. C. & Bogert, B. P. A dynamic theory of the cochlea. *J. Acoust. Soc. Am.* **22**, 369–381 (1950).
3. Zwislocki, J. J. Wave motion in the cochlea caused by bone conduction. *J. Acoust. Soc. Am.* **25**, 986–989 (1953).
4. Olson, E. S. Intracochlear pressure measurements related to cochlear tuning. *J. Acoust. Soc. Am.* **110**, 349–367 (2001).
5. Yoon, Y. J., Puria, S. & Steele, C. R. Intracochlear pressure and derived quantities from a three-dimensional model. *J. Acoust. Soc. Am.* **122**, 952–966 (2007).
6. Zinn, C., Maier, H., Zenner, H. & Gummer, A. W. Evidence for active, nonlinear, negative feedback in the vibration response of the apical region of the in-vivo guinea-pig cochlea. *Hear. Res.* **142**, 159–183 (2000).
7. Gold, T. Hearing. II. The physical basis of the action of the cochlea. *Proceedings of the Royal Society of London, Series B, Biological Sciences* **135**, 492–498 (1948).
8. Davis, H. An active process in cochlear mechanics. *Hear. Res.* **9**, 79–90 (1983).
9. Neely, S. T. & Kim, D. O. An active cochlear model showing sharp tuning and high sensitivity. *Hear. Res.* **9**, 123–130 (1983).
10. de Boer, E. Power amplification in an active model of the cochlea--short-wave case. *J. Acoust. Soc. Am.* **73**, 577–579 (1983).
11. Brownell, W. E., Bader, C. R., Bertrand, D. & de Ribaupierre, Y. Evoked mechanical responses of isolated cochlear outer hair cells. *Science* **227**, 194–196 (1985).
12. Dallos, P. The active cochlea. *J. Neurosci.* **12**, 4575–4585 (1992).
13. Robles, L. & Ruggero, M. A. Mechanics of the mammalian cochlea. *Physiological reviews* **81**, 1305–1352 (2001).
14. Hudspeth, A. J. How hearing happens. *Neuron* **19**, 947–950 (1997).
15. Ashmore, J. *et al.* The remarkable cochlear amplifier. *Hear. Res.* **266**, 1–17 (2010).
16. Fettiplace, R. & Hackney, C. M. The sensory and motor roles of auditory hair cells. *Nat. Rev. Neurosci.* **7**, 19–29 (2006).
17. Kemp, D. T. Stimulated acoustic emissions from within the human auditory system. *J. Acoust. Soc. Am.* **64**, 1386–1391 (1978).
18. Shera, C. A. & Guinan, J. J., Jr. Evoked otoacoustic emissions arise by two fundamentally different mechanisms: a taxonomy for mammalian OAEs. *J. Acoust. Soc. Am.* **105**, 782–798 (1999).
19. Meenderink, S. W. & van der Heijden, M. Reverse cochlear propagation in the intact cochlea of the gerbil: evidence for slow traveling waves. *J. Neurophysiol.* **103**, 1448–1455 (2010).
20. Dong, W. & Olson, E. S. Supporting evidence for reverse cochlear traveling waves. *J. Acoust. Soc. Am.* **123**, 222–240 (2008).
21. de Boer, E. & Nuttall, A. L. Inverse-solution method for a class of non-classical cochlear models. *J. Acoust. Soc. Am.* **125**, 2146–2154 (2009).
22. Wilson, J. P. Model for cochlear echoes and tinnitus based on an observed electrical correlate. *Hear. Res.* **2**, 527–532 (1980).
23. Ren, T. Reverse propagation of sound in the gerbil cochlea. *Nat. Neurosci.* **7**, 333–334 (2004).
24. Ruggero, M. A. Comparison of group delays of 2f1–f2 distortion product otoacoustic emissions and cochlear travel times. *ARLO* **5**, 143–147 (2004).
25. Siegel, J. H. *et al.* Delays of stimulus-frequency otoacoustic emissions and cochlear vibrations contradict the theory of coherent reflection filtering. *J. Acoust. Soc. Am.* **118**, 2434–2443 (2005).
26. Avan, P., Magnan, P., Smurzynski, J., Probst, R. & Dancer, A. Direct evidence of cubic difference tone propagation by intracochlear acoustic pressure measurements in the guinea-pig. *Eur. J. Neurosci.* **10**, 1764–1770 (1998).
27. Kimberley, B. P., Brown, D. K. & Eggermont, J. J. Measuring human cochlear traveling wave delay using distortion product emission phase responses. *J. Acoust. Soc. Am.* **94**, 1343–1350 (1993).
28. Mahoney, C. F. & Kemp, D. T. Distortion product otoacoustic emission delay measurement in human ears. *J. Acoust. Soc. Am.* **97**, 3721–3735 (1995).
29. Schneider, S., Prijs, V. F. & Schoonhoven, R. Group delays of distortion product otoacoustic emissions in the guinea pig. *J. Acoust. Soc. Am.* **105**, 2722–2730 (1999).
30. Schoonhoven, R., Prijs, V. F. & Schneider, S. DPOAE group delays versus electrophysiological measures of cochlear delay in normal human ears. *J. Acoust. Soc. Am.* **109**, 1503–1512 (2001).
31. He, W., Nuttall, A. L. & Ren, T. Two-tone distortion at different longitudinal locations on the basilar membrane. *Hear. Res.* **228**, 112–122, doi:10.1016/j.heares.2007.01.026 (2007).
32. He, W., Fridberger, A., Porsov, E., Grosh, K. & Ren, T. Reverse wave propagation in the cochlea. *Proc. Natl. Acad. Sci. USA.* **105**, 2729–2733 (2008).
33. de Boer, E., Zheng, J., Porsov, E. & Nuttall, A. L. Inverted direction of wave propagation (IDWP) in the cochlea. *J. Acoust. Soc. Am.* **123**, 1513–1521 (2008).
34. Vetesnik, A. & Gummer, A. W. Transmission of cochlear distortion products as slow waves: A comparison of experimental and model data. *J. Acoust. Soc. Am.* **131**, 3914–3934 (2012).
35. Sisto, R., Moleti, A., Botti, T., Bertaccini, D. & Shera, C. A. Distortion products and backward-traveling waves in nonlinear active models of the cochlea. *J. Acoust. Soc. Am.* **129**, 3141–3152 (2011).
36. Li, Y. & Grosh, K. Direction of wave propagation in the cochlea for internally excited basilar membrane. *J. Acoust. Soc. Am.* **131**, 4710–4721 (2012).
37. Hubbard, A. E. & Mountain, D. C. Alternating current delivered into the scala media alters sound pressure at the eardrum. *Science* **222**, 510–512 (1982).

38. Nakajima, H. H., Olson, E. S., Mountain, D. C. & Hubbard, A. E. Electrically evoked otoacoustic emissions from the apical turns of the gerbil cochlea. *J. Acoust. Soc. Am.* **96**, 786–794 (1994).

39. Ren, T. & Nuttall, A. L. Extracochlear electrically evoked otoacoustic emissions: a model for in vivo assessment of outer hair cell electromotility. *Hear. Res.* **92**, 178–183 (1995).

40. Nuttall, A. L. & Ren, T. Electromotile hearing: evidence from basilar membrane motion and otoacoustic emissions. *Hear. Res.* **92**, 170–177 (1995).

41. Rhode, W. S. Observations of the vibration of the basilar membrane in squirrel monkeys using the Mossbauer technique. *J. Acoust. Soc. Am.* **49**, 1218–1231 (1971).

42. Ruggero, M. A. & Rich, N. C. Application of a commercially-manufactured Doppler-shift laser velocimeter to the measurement of basilar-membrane vibration. *Hear. Res.* **51**, 215–230 (1991).

43. Nuttall, A. L., Dolan, D. F. & Avinash, G. Laser Doppler velocimetry of basilar membrane vibration. *Hear. Res.* **51**, 203–213 (1991).

44. Cooper, N. P. & Rhode, W. S. Basilar membrane tonotopicity in the hook region of the cat cochlea. *Hear. Res.* **63**, 191–196 (1992).

45. Russell, I. J. *et al.* Sharpened cochlear tuning in a mouse with a genetically modified tectorial membrane. *Nat. Neurosci.* **10**, 215–223 (2007).

46. Versteegh, C. P. & van der Heijden, M. Basilar Membrane Responses to Tones and Tone Complexes: Nonlinear Effects of Stimulus Intensity. *J. Assoc. Res. Otolaryngol.* (2012).

47. Ren, T., He, W. & Porsov, E. Localization of the cochlear amplifier in living sensitive ears. *PLoS One* **6**, e20149 (2011).

48. Ren, T. Longitudinal pattern of basilar membrane vibration in the sensitive cochlea. *Proc. Natl. Acad. Sci. USA.* **99**, 17101–17106 (2002).

49. Ren, T., He, W. & Gillespie, P. G. Measurement of cochlear power gain in the sensitive gerbil ear. *Nat Commun* **2**, 216 (2011).

50. Muller, M. The cochlear place-frequency map of the adult and developing Mongolian gerbil. *Hear. Res.* **94**, 148–156 (1996).

51. Martin, P. & Hudspeth, A. J. Active hair-bundle movements can amplify a hair cell's response to oscillatory mechanical stimuli. *Proc. Natl. Acad. Sci. USA.* **96**, 14306–14311 (1999).

52. Ricci, A. Active hair bundle movements and the cochlear amplifier. *J Am Acad Audiol* **14**, 325–338 (2003).

53. Xue, S., Mountain, D. C. & Hubbard, A. E. Electrically evoked basilar membrane motion. *J. Acoust. Soc. Am.* **97**, 3030–3041 (1995).

54. Grosh, K., Zheng, J., Zou, Y., de Boer, E. & Nuttall, A. L. High-frequency electromotile responses in the cochlea. *J. Acoust. Soc. Am.* **115**, 2178–2184 (2004).

55. Ren, T. Acoustic modulation of electrically evoked distortion product otoacoustic emissions in gerbil cochlea. *Neurosci. letters* **207**, 167–170 (1996).

56. Kirk, D. L. & Yates, G. K. Frequency tuning and acoustic enhancement of electrically evoked otoacoustic emissions in the guinea pig cochlea. *J. Acoust. Soc. Am.* **100**, 3714–3725 (1996).

57. Frank, G., Hemmert, W. & Gummer, A. W. Limiting dynamics of high-frequency electromechanical transduction of outer hair cells. *Proc. Natl. Acad. Sci. USA.* **96**, 4420–4425 (1999).

58. Ren, T., Guo, M., He, W., Miller, J. M. & Nuttall, A. L. Electrically evoked auditory nerve responses in the cochlea with normal outer hair cells. *J. Otol.* **4**, 71–75 (2009).

59. Zou, Y., Zheng, J., Nuttall, A. L. & Ren, T. The sources of electrically evoked otoacoustic emissions. *Hear. Res.* **180**, 91–100 (2003).

60. Fisher, J. A., Nim, F., Reichenbach, T., Uthaiah, R. C. & Hudspeth, A. J. The spatial pattern of cochlear amplification. *Neuron* **76**, 989–997 (2012).

61. Ruggero, M. A. & Rich, N. C. Furosemide alters organ of corti mechanics: evidence for feedback of outer hair cells upon the basilar membrane. *J. Neurosci.* **11**, 1057–1067 (1991).

62. Reichenbach, T., Stefanovic, A., Nin, F. & Hudspeth, A. J. Waves on Reissner's membrane: a mechanism for the propagation of otoacoustic emissions from the cochlea. *Cell reports* **1**, 374–384 (2012).

63. Ren, T. & Nuttall, A. L. Basilar membrane vibration in the basal turn of the sensitive gerbil cochlea. *Hear. Res.* **151**, 48–60 (2001).

64. Rhode, W. S. Basilar membrane mechanics in the 6–9 kHz region of sensitive chinchilla cochleae. *J. Acoust. Soc. Am.* **121**, 2792–2804 (2007).

Acknowledgments

Author contributions

W.H. and T.R. conceived the idea, planned the experiments, analyzed the data, and wrote the paper.

Additional information